1982 *Inorg. Chem.* **1999,** *38,* 1982−1988

# Mixed-Oxidation Divanadium(IV,V) Compound with Ligand Asymmetry: Electronic and Molecular Structure in Solution and in the Solid State

**Subodh Kanti Dutta,[†] Satyabrata Samanta,[†] Sujit Baran Kumar,[†] Oc Hee Han,[‡] Pannee Burckel,[§] A. Alan Pinkerton,[§] and Muktimoy Chaudhury*,[†]**

Department of Inorganic Chemistry, Indian Association for the Cultivation of Science,
Calcutta 700 032, India, Magnetic Resonance Group, Korea Basic Science Institute,
Yeueun-dong 52, Yoosung-goo, Taejeon, 305-333, South Korea, and Department of Chemistry,
College of Arts and Sciences, The University of Toledo, Toledo, Ohio 43606-3390

*Received June 30, 1998*

Reaction of $[V^{IV}OL^1(Im)]$ ($H_2L^1$ = *S*-methyl-3-((2-hydroxyphenyl)methyl)dithiocarbazate) with $[V^VOL(OCH_3)]$ allows isolation of $(ImH)[L^1OV\text{-}(\mu\text{-}O)\text{-}VOL]$ complexes **2** ($H_2L = H_2L^2$ = *S*-methyl-3-((5-bromo-2-hydroxyphenyl)methyl)dithiocarbazate) and **3** ($H_2L = H_2L^1$), one of which (**2**) has ligand asymmetry not previously known in this type of complex. In the solid state, $(ImH)[L^1OV\text{-}(\mu\text{-}O)\text{-}VOL^2]$ (**2**) provides an example of a divanadium(IV,V) compound with a syn angular $[V_2O_3]^{3+}$ core structure that exhibits crystallographically imposed mirror symmetry due to static disorder. Crystals of **2** are orthorhombic, space group *Pnma*, with $a = 10.740(2)$ Å, $b = 18.912(4)$ Å, $c = 17.163(4)$ Å, and $Z = 4$. In toluene at room temperature, both **2** and **3** have 8-line EPR spectra, characteristic of trapped-valence structure. When acetonitrile is added to these solutions, the spectra reveal 15-line features with asymmetric distortions that smooth out with the lowering of temperature. This probably has its origin in a solvent-dependent equilibrium involving two magnetically inequivalent structural forms of the divanadium(IV,V) compound, with syn angular and anti linear structures of the $[V_2O_3]^{3+}$ core. Variable temperatures (298−220 K) $^{51}V$ NMR spectroscopic studies in solution also support this view. In acetonitrile, both **2** and **3** exhibit an intervalence transfer band in the near-IR region at ca. 970 nm ($\epsilon$, 1600 and 1480 $M^{-1}$ $cm^{-1}$ for **2** and **3**, respectively) and they undergo one-electron reversible oxidation at ca. 0.40 V (vs SCE) due to the $V^{IV}V^V/V^VV^V$ couple.

## Introduction

The study of mixed-valence vanadium chemistry is an area of contemporary research interest.[1,2] Among the various types of mixed-oxidation compounds reported so far, dinuclear oxovanadium(IV,V) species containing the $[V_2O_3]^{3+}$ core represent the largest class because of their favorable thermodynamic stability and ease of formation from the constituent $[V^{1V}O]^{2+}$ and $[V^VO_2]^+$ ions.[3] Nishizawa et al.[4] was the first to report the crystal structure of a ($\mu$-oxo)divanadium(IV,V) compound $(NH_4)_3[V_2O_3(nta)_2]\cdot 3H_2O$,[5] prepared by the metathesis of the constituent $[V^VO_2(nta)]^{2-}$ and $[V^{IV}O(nta)]^-$ anions. The structure of the addition product shows the presence of a dioxo $\mu$-oxo core with an anti linear structure as shown in Figure 1a. Since then, many other dioxovanadium(IV,V) compounds have been reported, showing diversity in their electronic and molecular structures[6−13] (Figure 1). The majority of these compounds,[4,6−8] however, have almost a linear V−O−V bridge with the terminal oxo groups in mutually trans positions (Figure 1a), allowing significant overlap of the $d_{xy}$ metal orbitals across

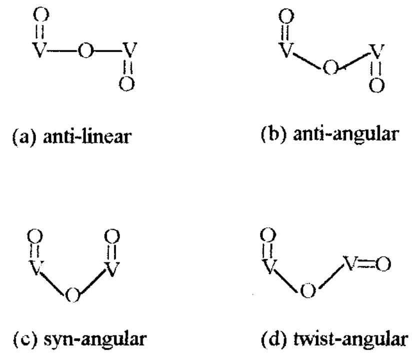
(a) anti-linear
(b) anti-angular
(c) syn-angular
(d) twist-angular

**Figure 1.** Possible configurations of the bridging and terminal oxygen atoms in $[V_2O_3]^{3+}$ core, found in the $\mu$-oxo divanadium(IV,V) complexes.

---

[†] Indian Association for the Cultivation of Science.

[‡] Korea Basic Science Institute.

[§] The University of Toledo.

(1) Boas, L. V.; Pessoa, J. C. In *Comprehensive Coordination Chemistry*; Wilkinson, G., Ed.; Pergamon: Oxford, 1987; Vol. 3, p 453.

(2) Young, C. G. *Coord. Chem. Rev.* **1989**, *96*, 89.

(3) Blanc, P.; Madic, C.; Launay, J.-P. *Inorg. Chem.* **1982**, *21*, 2923.

(4) Nishizawa, M.; Hirotsu, K.; Ooi, S.; Saito, K. *J. Chem. Soc., Chem. Commun.* **1979**, 707.

(5) Abbreviations used: nta = nitrilotriacetate; *S*-peida = (*S*)-[[1-(2-pyridyl)ethyl]imino]diacetate; salser = *N*-salicylidene serinate; alsal = salicylidene alaninate; $H_2L^1$ = 3-((2-hydroxyphenyl)methyl)-dithiocarbazate; $H_2L^2$ = 3-((2-hydroxy-5-bromophenyl)methyl)dithiocarbazate; BzIm = benzimidazole; Im = imidazole; tpa = *tris*-(2-pyridylmethyl)amine; TEAP = tetraethylammonium perchlorate.

(6) (a) Launay, J.-P.; Jeannin, Y.; Daoudi, M. *Inorg. Chem.* **1985**, *24*, 1052. (b) Babonneau, F.; Sanchez, C.; Livage, J.; Launay, J.-P.; Daoudi, M.; Jeannin, Y. *Nouv. J. Chim.* **1982**, *6*, 353.

(7) Holwerda, R. A.; Whittlesey, B. R.; Nilges, M. J. *Inorg. Chem.* **1998**, *37*, 64.

(8) Mahroof-Tahir, M.; Keramidas, A. D.; Goldfarb, R. B.; Anderson, O. P.; Miller, M. M.; Crans, D. C. *Inorg. Chem.* **1997**, *36*, 1657.

(9) (a) Kojima. A.; Okazaki. K.; Ooi, S.; Saito, K. *Inorg. Chem.* **1983**, *22*, 1168. (b) Okazaki, K.; Saito, K. *Bull. Chem. Soc. Jpn.* **1982**, *55*, 785.

(10) Schulz, D.; Weyhermüller, T.; Wieghardt, K.; Nuber, B. *Inorg. Chim. Acta* **1995**, *240*, 217.

10.1021/ic980743+ CCC: $18.00

the oxo bridge. This generates a situation where the odd electron is efficiently delocalized between the two vanadium centers, as confirmed by X-ray crystallography. Among this type, the only exception is Na[$V_2O_3$(*S*-peida)$_2$]·$NaClO_4$·$H_2O$, which, despite its perfectly anti linear structure (V−O−V, 179.5°), has two crystallographically different vanadium centers.[9]

A second category of compounds with anti angular core structures has been reported recently by Wieghardt et al.,[10] in which the V−O−V bridge is bent and the two terminal V=O groups are nearly trans to each other (Figure 1b). Both trapped-valence and delocalized electronic structures are found in complexes with this type of core, depending on the $\pi$ donor ability of the ligands in the equatorial plane. Pessoa et al.[11] have recently reported a third type of $V_2O_3$ structure involving a syn angular core with bent V−O−V (146.6°) bridge (Figure 1c). The compound Na[$V_2O_3$(DL-salser)$_2$]·5$H_2O$ has a localized electronic structure in the solid state apparently due to insignificant overlap of the symmetry-constrained $d_{xy}$ metal orbitals. A fourth type of $[V_2O_3]^{3+}$ core with a twist angular configuration has been observed in the complex $Et_4N$[$V_2O_3$(L-alsal)$_2$][12] where the relative disposition of the two V=O groups is intermediate between the syn and anti forms (Figure 1d) with localized electronic structure. The V−O−V angle (113.2°) is by far the smallest observed in any such compound. All these complexes are made up of ligands having O/N donor atom sets and in solution, with a few exceptions,[10,14] have a delocalized electronic structure (class II or III)[15] on the time scale of EPR spectroscopy.[16]

Over the past few years we have been working on the coordination chemistry of oxometalate ions in sulfur donor environments.[13,17,18] The observed flexibility and diversity in the electronic and molecular structures of the dinuclear complexes containing the $[V_2O_3]^{3+}$ core have prompted us to synthesize the $\mu$-oxo divanadium(IV,V) compound (BzImH)-[$L^1$OV-($\mu$-O)-VO$L^1$] (**1**)[13] using the tridentate ONS donor ligand *S*-methyl-3-((2-hydroxyphenyl)methyl)dithiocarbazate ($H_2L^1$). Compound **1** has a syn angular core structure (Figure 1c) with a bent (144.0(6)°) V−O−V bridge. It has a trapped-valence structure in the solid state but reveals a 15-line EPR spectrum in acetonitrile solution at room temperature, indicating delocalization of the odd electron between the participating vanadium centers on the time scale of EPR spectroscopy.

In all mixed-oxidation divanadium(IV,V) compounds reported so far, the metal centers have symmetrical ligand environments. Herein, we report the synthesis of a compound (ImH)[$L^1$OV-($\mu$-O)-VO$L^2$] (**2**), containing two dissimilar tridentate ONS ligands, $H_2L^1$ and its bromo derivative $H_2L^2$, bound to the metal centers. X-ray crystallography, FT-IR, EPR, and $^{51}$V NMR spectroscopic studies were made to understand the electronic and molecular structures of this and similar compounds in the solid state and in solution.

## Experimental Section

Unless otherwise stated, all reactions were carried out under an atmosphere of purified dinitrogen. Solvents were reagent grade, dried by standard methods,[19] and distilled under nitrogen prior to their use. Tridentate ligands $H_2L^1$ and $H_2L^2$, precursor complexes [VO$L^1$(Im)] and [VO$L^1$($OCH_3$)] and the mixed-oxidation compound (BzImH)[$L^1$-OV-($\mu$-O)-VO$L^1$] (**1**) were prepared as previously described.[13,18] [VO-(acac)$_2$] was prepared following a literature method[20] and [VO$L^2$-($OCH_3$)], the same procedure as for [VO$L^1$($OCH_3$)][13] was adopted. All other reagents were commercially available and used as received.

**Syntheses. (ImH)[$L^1$OV-($\mu$-O)-VO$L^2$]·$CH_3COCH_3$·$H_2O$ (2).** A suspension of [VO$L^1$(Im)] (0.18 g, 0.50 mmol) and [VO$L^2$($OCH_3$)] (0.20 g, 0.50 mmol) in acetone (20 mL) was stirred at room temperature for ca. 2 h to give a green solution. It was filtered and the filtrate was stored at 0 °C overnight, yielding a dark green microcrystalline solid. The product was collected on a glass frit, washed with $Et_2O$ (2 × 5 mL) and dried *in vacuo*. Black crystals of **2** (some of which were of good X-ray quality) were obtained by layering hexanes carefully over an acetone solution of the compound at 0 °C. Yield: 80 mg (20%). Anal. Calcd for $V_2C_{24}H_{28}N_6O_7S_4Br$: C, 35.03; H, 3.40; N, 10.22. Found: C, 34.7; H, 3.2; N, 10.2%. IR (KBr disk), cm$^{-1}$: $\nu$(C$\overset{...}{-}$N), 1600 s; $\nu$(C=C/aromatic), 1540 s; $\nu$(V=$O_t$), 978 s; $\nu_{asym}$(V−O−V), 826 m. UV−vis ($CH_3CN$), $\lambda_{max}$, nm ($\epsilon$, M$^{-1}$ cm$^{-1}$): 965 (1600); 750 (sh, 950); 396 (15 500); 288 (32 400); 231 (48 200). $\mu_{eff}$ (solid, 25 °C): 1.65 $\mu_B$.

**(ImH)[$L^1$OV-($\mu$-O)-VO$L^1$] (3).** To a stirred suspension of [VO$L^1$-(Im)] (0.18 g, 0.50 mmol) in acetonitrile (20 mL) was added an equimolar amount (0.16 g, 0.50 mmol) of solid [VO$L^1$($OCH_3$)]. Stirring was continued for ca. 2 h, when a green solution was obtained. The solution was filtered and the filtrate on standing overnight at 0 °C gave crystalline flakes of **3**. Yield: 0.1 g (30%). Anal. Calcd for $V_2C_{21}H_{21}N_6O_5S_4$: C, 37.78; H, 3.15; N, 12.59. Found: C, 37.7; H, 3.1; N, 12.9. IR (KBr disk), cm$^{-1}$: $\nu$(C$\overset{...}{-}$N), 1600 s; $\nu$(C=C/aromatic), 1545 s; $\nu$(V=$O_t$), 980 s; $\nu_{asym}$(V−O−V), 830 m. UV−vis ($CH_3CN$), $\lambda_{max}$, nm ($\epsilon$, M$^{-1}$ cm$^{-1}$): 970 (1480); 740 (sh, 900); 389 (14 300); 298 (37 000); 227 (46 300). $\mu_{eff}$ (solid, 25 °C), 1.68 $\mu_B$.

Attempts to grow diffraction quality crystals of this compound were not successful.

**Physical Measurements.** EPR spectra in solution at variable temperatures were recorded in the X-band on a Bruker model ESP 300E spectrometer. Electronic spectra in the near-IR region were obtained on a Hitachi U-3400 UV/Vis/near-IR spectrometer and IR spectra (as KBr disk) using a Nicolet Magna 750 FT-IR spectrometer. Room-temperature magnetic moments and UV−vis spectra were obtained as described elsewhere.[13,17] Elemental analyses (for C, H, and N) were performed in this laboratory (at IACS) using a Perkin-Elmer 2400 analyzer.

$^{51}$V NMR spectra at variable temperatures (298−220 K) were recorded in solution ($CD_3CN$/toluene, 1:2 v/v) using a Varian UNITY plus 300 instrument equipped with a broad band probe and a decoupling channel. A Larmor frequency of 78.90 MHz, spectral width of 60 kHz, and acquisition time of 320 ms were employed. A pulse length of 11.5 $\mu$s corresponding to a 90° flip angle with a 2 s pulse repetition delay were used. Chemical shifts are referenced to external neat $VOCl_3$ and the precision of the chemical shifts is ±1 ppm.

Cyclic voltammetry was performed in acetonitrile solution with a PAR model 362 scanning potentiostat using Pt working and auxiliary electrodes and 0.1 M TEAP as the supporting electrolyte; potentials are referenced to the SCE. Bulk electrolysis was carried out using a Pt-gauze working electrode. The ferrocene/ferrocenium (Fc/Fc$^+$) couple was used as the internal standard.[21]

**X-ray Crystallography.** A black, suitable crystal of **2** with dimensions 0.40 × 0.40 × 0.40 mm was mounted on a glass fiber and used

---

(11) Pessoa, J. C.; Silva, J. A. L.; Vieira, A. L.; Vilas-Boas, L.; O'Brien, P.; Thornton, P. *J. Chem. Soc., Dalton Trans.* **1992**, 1745.

(12) Mondal, S.; Ghosh, P.; Chakravorty, A. *Inorg. Chem.* **1997**, *36*, 59.

(13) Dutta, S. K.; Kumar, S. B.; Bhattacharyya, S.; Tiekink, E. R. T.; Chaudhury, M. *Inorg. Chem.* **1997**, *36*, 4954.

(14) Oyaizu et al. (Oyaizu, K.; Yamamoto, K.; Yoneda, K.; Tsuchida, E. *Inorg. Chem.* **1996**, *35*, 6634) have recently reported a divanadium-(IV,V) compound [(salen)$V^{IV}$-O-$V^{V}$O(salen)]$I_3$, containing $[V_2O_2]^{5+}$ core that exhibits an eight-line EPR in $CH_2Cl_2$ solution at room temperature.

(15) Robin, M. B.; Day, P. *Adv. Inorg. Chem. Radiochem.* **1967**, *10*, 247.

(16) EPR spectrum of the compound Na[$V_2O_3$(DL-salser)$_2$]·5$H_2O$ was not reported in the literature (see ref 11).

(17) Dutta, S. K.; McConville, D. B.; Youngs, W. J.; Chaudhury, M. *Inorg. Chem.* **1997**, *36*, 2517 and references therein.

(18) Dutta, S. K.; Tiekink, E. R. T.; Chaudhury, M. *Polyhedron* **1997**, *16*, 1863.

(19) Perrin, D. D.; Armarego, W. L. F.; Perrin, D. R. *Purification of Laboratory Chemicals*, 2nd ed.; Pergamon: Oxford, England, 1980.

(20) Rowe, R. A.; Jones, M. M. *Inorg. Synth.* **1957**, *5*, 113.

(21) Gagné, R. R.; Koval, C. A.; Lisensky, G. C. *Inorg. Chem.* **1980**, *19*, 2854.

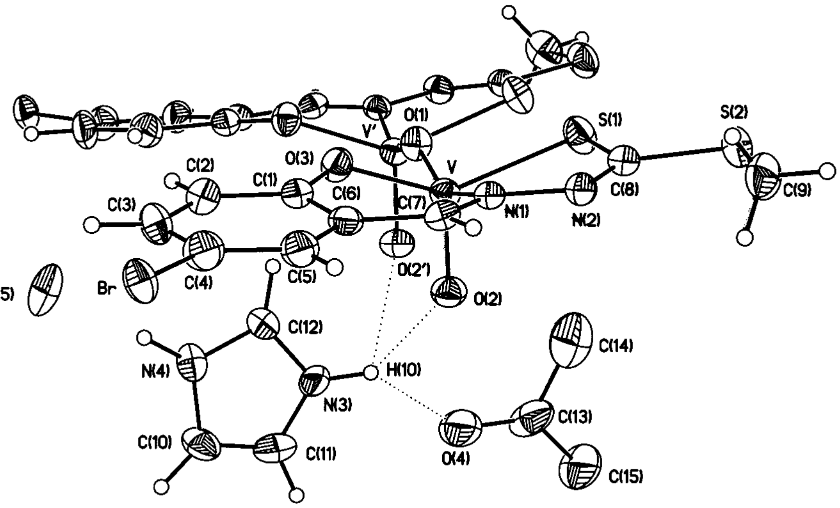

**Figure 2.** Molecular structure of (ImH)[L$^1$OV-($\mu$-O)-VOL$^2$]·$CH_3COCH_3$·$H_2O$ (**2**) showing the atom-labeling scheme. All atoms are represented by 20% probability thermal ellipsoids. The Br atom is shown at two ligand sites corresponding to the one-half disorder model.

**Table 1.** Summary of Crystallographic Data for (ImH)[L$^1$OV-($\mu$-O)-VOL$^2$] (**2**)

| | |
|---|---|
| empirical formula | $C_{24}H_{28}BrN_6O_7S_4V_2$ |
| fw | 822.58 |
| space group | orthorhombic, *Pnma* (No. 62) |
| $a$, Å | 10.740(2) |
| $b$, Å | 18.912(4) |
| $c$, Å | 17.163(4) |
| $V$, Å$^3$ | 3486(2) |
| $Z$ | 4 |
| $T$, K | 294 ± 1 |
| $\lambda$ (Mo Kα), Å | 0.710 73 |
| $\rho_{calcd}$, g cm$^{-3}$ | 1.57 |
| $\mu$, cm$^{-1}$ | 19.3 |
| $R^a$ | 0.065 |
| $R_w{}^b$ | 0.087 |

$^a$ $R = \sum(|F_o| - |F_c|)/\sum|F_o|$. $^b$ $R_w = [\sum w(|F_o| - |F_c|)^2/\sum w(|F_o|^2)]^{1/2}$.

**Table 2.** Selected Bond Lengths (Å) and Angles (deg) for (ImH)[L$^1$OV-($\mu$-O)-VOL$^2$] (**2**)

| Distances (Å) | | | |
|---|---|---|---|
| V−O(2) | 1.590(4) | V−N(1) | 2.109(5) |
| V−O(1) | 1.801(2) | V−S(1) | 2.339(2) |
| V−O(3) | 1.898(4) | C(8)−S(1) | 1.716(7) |

| Angles (deg) | | | |
|---|---|---|---|
| S(1)−V−O(1) | 88.7(2) | O(1)−V−N(1) | 154.3(2) |
| S(1)−V−O(2) | 109.1(2) | O(2)−V−O(3) | 109.9(2) |
| S(1)−V−O(3) | 139.3(1) | O(2)−V−N(1) | 98.5(2) |
| S(1)−V−N(1) | 79.0(1) | O(3)−V−N(1) | 84.2(2) |
| O(1)−V−O(2) | 106.8(2) | C(1)−O(3)−V | 129.7(4) |
| O(1)−V−O(3) | 91.0(2) | V−O(1)−V$^1$ | 149.7(4) |

for data collection at 21 ± 1 °C in $\omega-2\theta$ scan mode on an Enraf-Nonius CAD-4 diffractometer equipped with graphite monochromatized Mo Kα ($\lambda$ = 0.710 73 Å) radiation. No crystal decay was observed during the data collection. The unit cell parameters were obtained by least-squares refinement of the angular settings from 25 reflections in the $2\theta$ range of 12−28°. Relevant crystallographic data are given in Table 1, and selected bond lengths and angles in Table 2.

Data were corrected for Lorentz and polarization effects. An empirical absorption (from 0.814 to 1.000 on I) correction was also applied. The maximum $2\theta$ value for data collection was 52.0°. The number of measured reflections was 3850, all of which were unique. The structure was solved by direct methods (SIR-92)[22] followed by full-matrix least-squares refinement of the function $\sum\omega(|F_o| - |F_c|)^2$, where $\omega = 4F_o^2/\sigma^2(F_o^2)$. The complex anion lies across the crystallographic mirror plane, thus the bromine atom is disordered over the two ligand sites. Consistent with the chemical analysis, one molecule each of water and acetone from the crystallization solvents were found to be present in the unit cell. The countercation $[C_3N_2H_5]^+$ and the solvent molecules $(CH_3)_2CO$ and $H_2O$ are also disordered across the mirror plane. These atoms as well as the bromine atom in the complex anion were refined with one-half occupancy. All other non-hydrogen atoms were refined with anisotropic displacement parameters. Hydrogen atoms for the ordered part of the structure were refined as riding atoms, other hydrogen atoms were not included. Final $R$ and $R_w$ values are 0.065 and 0.087, respectively, and the goodness of fit ($s$) = 2.81 for 2119 unique reflections with $F_o^2 > 3.0\sigma(F_o^2)$ and 244 parameters. The final Fourier difference synthesis showed a maximum and minimum of +0.95 and −0.28 e/Å$^3$. All computations were performed by using MolEN.[23] Scattering factors were taken from the usual sources.[24] The atom labeling scheme employed is shown in Figure 2.

Attempts to refine this structure in the acentric space group were unsuccessful.

## Results and Discussion

**Synthesis.** All mixed-oxidation $\mu$-oxo divanadium(IV,V) compounds reported so far[4,6−12] have a common feature. They all have two molecules of the same O/N donor ligand, each coordinated to a metal center. These are obtained through (a) stoichiometric (1:1 mol ratio) mixing of preformed vanadium(V) and -(IV) precursor compounds,[4,6] (b) controlled oxidation[9−11] or reduction[8] of mononuclear vanadium(IV) or -(V) precursors, respectively, and (c) controlled oxidation (chemical)[7] or reduction (electrochemical)[12] of dinuclear isovalent species. In an earlier communication,[13] we have reported the synthesis of the mixed-oxidation compound (BzImH)[L$^1$OV-($\mu$-O)-VOL$^1$] (**1**) according to method (a) by reacting the precursors [V$^V$OL$^1$(OCH$_3$)] and [V$^{IV}$OL$^1$(BzIm)] in 1:1 molar ratio. Compound **1** has a trapped-valence structure in the solid state with a syn angular disposition of the $[V_2O_3]^{3+}$ core. We were intrigued to know whether, in the mixed-valence compound, the precursor

---

(22) Burla, M. C.; Camalli, M.; Cascarano, G.; Giacovazzo, C.; Polidori, G.; Spagna, R.; Viterbo, D. *J. Appl. Crystallogr.* **1989**, *22*, 389.

(23) Fair, C. K. *MolEN, An Interactive Intelligent System for Crystal Structure Analysis. User Manual*; Enraf-Nonius: Delft, The Netherlands, 1990.

(24) *International Tables for X-ray Crystallography*; Kynoch Press: Birmingham, England, 1974; Vol. IV (present distributor: Klewer Academic Publishers, Dordrecht, The Netherlands).

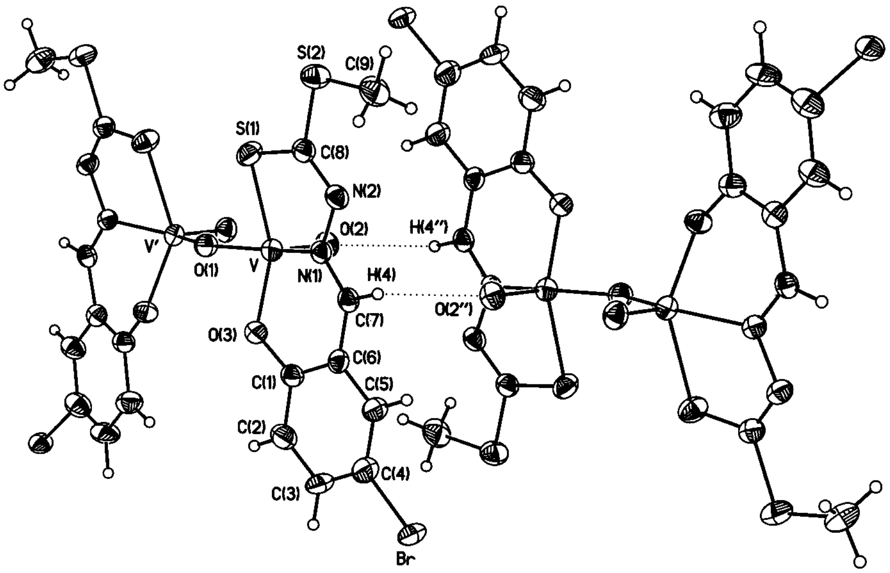

**Figure 3.** Drawing of the dimeric form of the anion showing hydrogen bonds between O(2) and H(4): C(7)−H(4)···O(2); 2.503(4) Å, 145.2(4)°. Counterion and solvent molecules are omitted for clarity.

vanadium complexes retain their initial oxidation states or, during reaction, valence crossover takes place to generate the trapped-valence species **1**, as shown in eq 1.

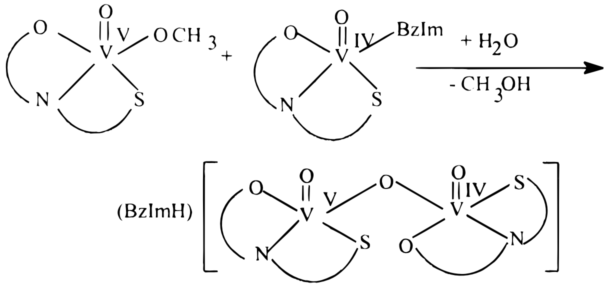

(1)

**1**

To address this and other questions regarding the electronic and molecular structures of mixed-valence divanadium(IV,V) compounds, we have now used the precursor compounds [$V^{IV}$-$OL^1$(Im)] and [$V^VOL^2(OCH_3)$] with two dissimilar ligands attached to the metal centers. The product (ImH)[$L^1$OV-($\mu$-O)-$VOL^2$] (**2**), to our knowledge, is the first mixed-oxidation divanadium(IV,V) compound containing two different ligand molecules coordinated to the vanadium centers. Unlike **1**, compound **2** surprisingly has apparent mirror symmetry in the solid state (see later). Another closely similar compound (ImH)-[$L^1$OV-($\mu$-O)-$VOL^1$] (**3**) with a symmetrical ligand system was also prepared for comparison. Both compounds **2** and **3** are dark green crystalline solids and have room-temperature magnetic moments of 1.65 (**2**) and 1.68 $\mu_B$ (**3**). In solution (except for DMF and $CH_2Cl_2$) they are fairly stable undergoing slow decomposition only on prolonged standing.

**Description of the Crystal Structure.** Figure 2 displays the molecular structure and the atom numbering scheme for compound **2**. Selected interatomic parameters are listed in Table 2. Unlike compound 1,[13] the dinuclear mixed-valence anion in **2** possesses crystallographic mirror symmetry with the bridging oxygen atom O(1) residing on the mirror plane. This indicates an apparent equivalence of the two LOV halves in the unsymmetrical [$L^1$ OV-($\mu$-O)-$VOL^2$ ]$^-$ anion of **2** due to a statistical distribution of the molecular forms [$L^1$OV-($\mu$-O)-$VOL^2$]$^-$ and [$L^2$OV-($\mu$-O)-$VOL^1$]$^-$ appearing in pair in the crystal lattice (Figure 3). Individual molecules in this pair are connected by intermolecular hydrogen bonds between O(2) and H(4): C(7)−H(4)···O(2), 2.503(4) Å (145.2(4)°). The vanadium centers have square-pyramidal geometry in which S(1), N(1), and O(3) of the tridentate ligand ($L^1$ or $L^2$) and the bridging oxygen O(1) define the equatorial plane; the metal center is displaced toward the apical oxo ligand O(2) by 0.565(1) Å.

The molecule has a bent V−O−V (149.7(4)°) bridge with a syn dioxo-$\mu$-oxo core structure for the $[V_2O_3]^{3+}$ group (Figure 1c). In the homoleptic anion [$L^1$OV-($\mu$-O)-$VOL^1$]$^-$ of **1**, the two vanadium atoms are crystallographically nonequivalent,[13] while in the heteroleptic anion [$L^1$OV-($\mu$-O)-$VOL^2$]$^-$ of **2**, due to the dimerization process as mentioned above, the positions of the two metal centers are averaged as indicated by the comparison of the relevant bond distances in **1** and **2**. Thus the bridging V−$O_b$ distance 1.801(2) Å observed in each half of **2** is equal to the average of the unequal V−$O_b$ distances 1.768(7) and 1.833(7) Å found in **1**. Similar agreement also holds true for the V−O(3) distances in **2** (1.898(4) Å) and **1** (1.880(9) and 2.080(9) Å).

A careful scrutiny of the structures of **1** and **2** reveals another subtle but interesting difference resulting from the relative arrangements of tridentate ligands. While in compound **1**[13] a trans disposition of the ligands is observed, the corresponding arrangement is found to be cis in **2**. The bromine atom in **2** is resolved with one-half occupancy shared between the two ligand sites, giving this molecule crystallographic mirror symmetry due to static disorder. The asymmetric unit of **2** contains one-half molecule each of solvent water (O(5) in Figure 2) and acetone. The imidazolium counterion and both these solvent molecules are also disordered across the mirror plane. There are weak hydrogen bonding interactions in **2** between H(10) of imidazolium cation to O(2) and O(2A) of the complex anion: N(3)−H(10)···O(2), 2.751(4) Å (111.0 ± 1.3°), and N(3)−H(10)···O(2A), 2.559(4) Å (112.5 ± 1.2°). Also there is a fairly strong hydrogen bond contact between the imidazolium proton H(10) and the carbonyl oxygen O(4) of the acetone molecule: N(3)−H(10)···O(4), 1.978(10) Å (139.20(7)°) as labeled in Figure 2.

From a survey of the available structural data for the mixed-oxidation divanadium compounds containing $[V_2O_3]^{3+}$ core,[4,6−13] several features emerge. Compounds with tetradentate ligands,[4,6−9] in general, have octahedral vanadium centers which are parts

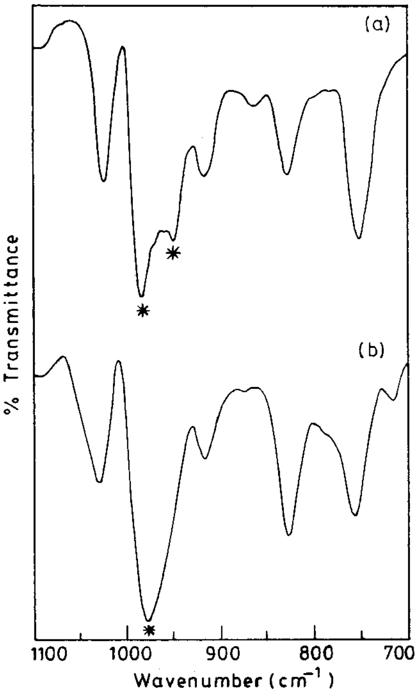

**Figure 4.** Relevant region (1100−700 cm$^{-1}$) of the IR spectra (in KBr disk) of **1** (a) and **2** (b), showing the nature of the $\nu$(V=O$_t$) stretching modes.

of an anti linear $[V_2O_3]^{3+}$ core (Figure 1a). On the other hand, with tridentate ligands, the vanadium centers have square pyramidal geometry that favors a syn angular core structure (Figure 1c) for the $[V_2O_3]^{3+}$ group.[11,13] However, departures from these general observations occur when there are strong steric demands from the coordinating ligands.[10,12]

**Infrared Spectroscopy.** The IR spectra of **2** and **3** display characteristic strong bands at 1600 and 1540 cm$^{-1}$ due to $\nu$(C⩦N) and $\nu$(C=C/aromatic) stretching modes of the coordinated ligands. The spectra of **1** and **2** in the range 1100−700 cm$^{-1}$ (shown in Figure 4) reveal interesting differences in their metal−oxygen vibrational modes. For compound **1** (Figure 4a), a pair of bands are observed at 984 and 950 cm$^{-1}$ for terminal $\nu$(V=O$_t$) stretches, while for **2** only a single such mode is detected at 978 cm$^{-1}$ (Figure 4b). This is in agreement with the unsymmetrical nature of the terminal V=O$_t$ bonds in **1** and provides an indication of the averaged structure in **2** due to possible static disordering in the dimeric structure (Figure 3).

**EPR Spectroscopy.** For mixed-oxidation divanadium(IV,V) complexes, EPR spectroscopy serves as an useful diagnostic tool to decide the state of localization of the unpaired electron. While the observation of a 15-line profile ($^{51}$V, $I = {}^7/_2$) gives a clear indication of the odd electron being coupled to both the participating vanadium centers,[4,6,7,12,13] an 8-line pattern, also observed in few cases,[8,10] suggests a valence-trapped situation for the odd electron on the time-scale of EPR spectroscopy. For both compounds **2** and **3**, almost identical spectra are obtained in CH$_3$CN/toluene (1:2 v/v) solution. Spectra of **2** at different temperatures are shown in Figure 5. It may be noted that the 15-line room-temperature spectrum ($\langle g\rangle$, 1.987 and $\langle A\rangle_{15}$, 44.8 × 10$^{-4}$ cm$^{-1}$) shows some asymmetric distortions and appreciable line-broadening (Figure 5a). Similar features were also observed in the spectrum of **1**.[13] Holwerda et al.[7] have explained this asymmetry as arising from incomplete motional averaging of the **g** tensor or hyperfine anisotropy. In that case, one would expect to see more pronounced spectral asymmetry at low temperature due to slower molecular tumbling. Contrary to this, the spectrum of **2** at low temperature (240 K) displays a more clear 15-line profile with reduced asymmetry (Figure 5b).

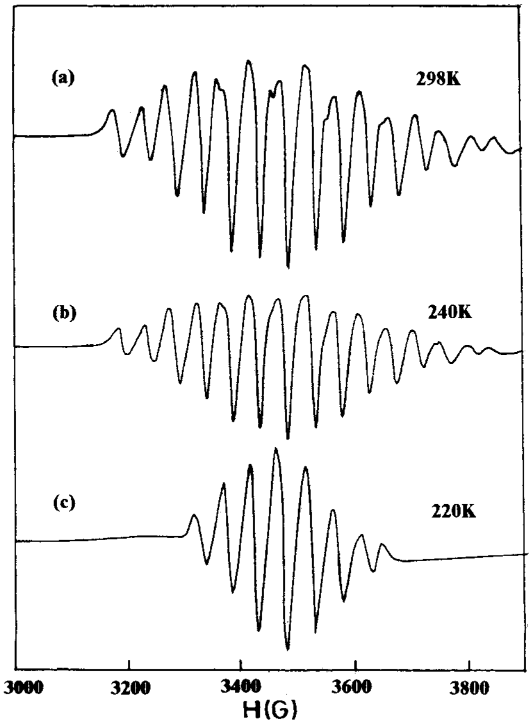

**Figure 5.** X-band EPR spectra of (ImH)[L$^1$OV-($\mu$-O)-VOL$^2$] (**2**) in CH$_3$CN/toluene (1:2 v/v) solution at variable temperatures.

The possible reason for this asymmetry, we believe, is a temperature-dependent equilibrium process involving more than one EPR active species. For a mixed-oxidation compound, one such process may involve a cross-electron-transfer reaction (eq 2), as observed by Myser and Shepherd[25] for a divanadium(III,IV) compound.

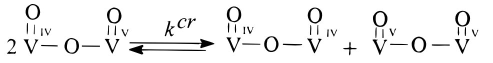

$$2\ \overset{\mathrm{O}}{\overset{\|}{\mathrm{V}}}{}^{\mathrm{IV}}\!-\mathrm{O}-\overset{\mathrm{O}}{\overset{\|}{\mathrm{V}}}{}^{\mathrm{V}}\ \overset{k^{cr}}{\rightleftharpoons}\ \overset{\mathrm{O}}{\overset{\|}{\mathrm{V}}}{}^{\mathrm{IV}}\!-\mathrm{O}-\overset{\mathrm{O}}{\overset{\|}{\mathrm{V}}}{}^{\mathrm{IV}} + \overset{\mathrm{O}}{\overset{\|}{\mathrm{V}}}{}^{\mathrm{V}}\!-\mathrm{O}-\overset{\mathrm{O}}{\overset{\|}{\mathrm{V}}}{}^{\mathrm{V}} \qquad (2)$$

The divanadium(IV,IV) compound containing the $[V_2O_3]^{2+}$ core proposed to be formed in the above reaction will, in all probability, be EPR inactive.[26] Moreover, such an equilibrium is not thermodynamically favored in the present system as both compounds **2** and **3** fail to generate the corresponding divanadium(IV,IV) counterparts by electrochemical reduction (see later).

Another possibility is a solvent dependent process as shown by eq 3. Compound **2** with square pyramidal vanadium centers, when dissolved in CH$_3$CN, may add up two molecules of solvent (S) to generate a species having octahedral vanadium centers with a concomitant change in the $[V_2O_3]^{3+}$ core structure from a syn angular to an anti linear mode (Figure 1). The linear V−O−V bridge allows effective interactions between the d$_{xy}$ metal orbitals via the p$\pi$ orbital of the bridging oxo atom.[2] On the other hand, a valence-trapped situation is normally encountered in molecules with a syn angular core structure due to poor overlap of the symmetry-constrained d$_{xy}$ metal orbitals.[11,13] Both these species in equilibrium are EPR active but magnetically

---

[25] Myser, T. K.; Shepherd, R. E. *Inorg. Chem.* **1987**, *26*, 1544.

[26] Toftlund et al. (Toftlund, H.; Larsen, S.; Murray, K. S. *Inorg. Chem.* **1991**, *30*, 3964.) have reported recently a divanadium(IV,IV) compound [(tpa)OV$^{IV}$-($\mu$-O)-V$^{IV}$O(tpa)](ClO$_4$)$_2$ which is diamagnetic due to strong antiferromagnetic coupling and is the only example of a structurally characterized compound containing $[V_2O_3]^{2+}$ core, reported so far in the literature.

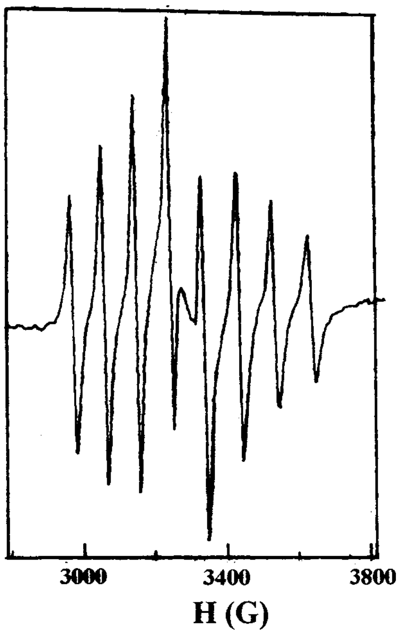

**Figure 6.** X-band EPR spectrum of (ImH)[L$^1$OV-($\mu$-O)-VOL$^2$] (**2**) in toluene solution at 298 K.

inequivalent due to their difference in stereochemical configurations. The spectral features observed at room temperature for **2** (shown in Figure 5a) appear to arise due to the superposition of the EPR spectra of two closely related species.

As the temperature is lowered, the equilibrium (eq 3) is likely

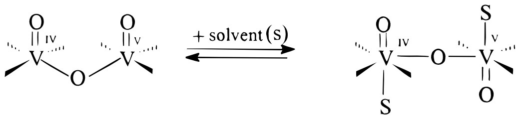

(3)

to be shifted more to the right-hand side. The spectrum at 240 K (Figure 5b) appears to have a more clear 15-line feature with some degree of broadening still there due to slower tumbling of the molecules at lower temperature. On further lowering of the temperature, the intramolecular thermal electron-transfer rate ($k_{th}$) decreases, resulting in a spectral coalescence from a 15-line to an 8-line feature at 220 K (Figure 5c) due to thermal trapping of the odd electron at one of the vanadium centers. Using an approximation as described in the literature,[27] the activation energy ($E^{\ddagger}$) and thermal electron-transfer rate ($k_{th}$) are estimated to be 3.95 kcal mol$^{-1}$ and 7.45 × 10$^8$ s$^{-1}$ (at 25 °C), respectively.

To test the validity of the proposed solvation hypothesis as described above, EPR spectra of the complexes **2** and **3** were further examined in neat toluene and propylene carbonate as solvents. In each case a clear 8-line pattern at $\langle g \rangle = 1.97$ with $\langle A \rangle_8 = 89 \times 10^{-4}$ cm$^{-1}$ is obtained at room temperature, as shown in Figure 6 for a representative compound (**2**). In the absence of any mononuclear vanadium(IV) species in solution (see later), this result indicates a valence-trapped situation for these mixed-oxidation complexes in noncoordinating solvents possibly due to bent $V_2O_3$ core structure as proposed in eq 3. Also as expected,[27,28] the average vanadium hyperfine splittings for the localized spectra ($\langle A \rangle_8$, $89 \times 10^{-4}$ cm$^{-1}$) are found to be twice as high as that of the delocalized spectra ($\langle A \rangle_{15}$, $44.8 \times 10^{-4}$ cm$^{-1}$) due to reasons already advanced by Slichter.[29]

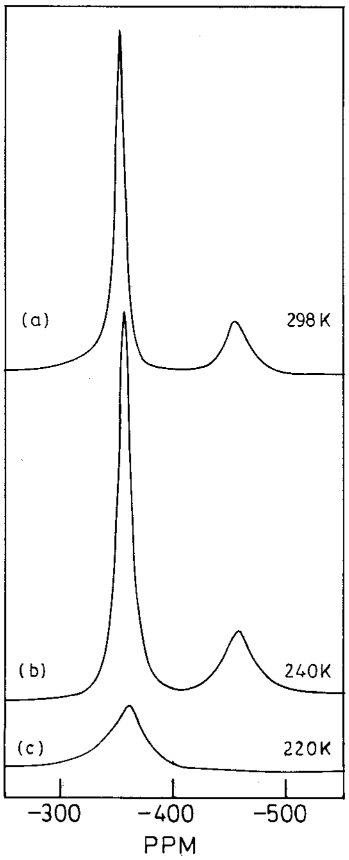

**Figure 7.** $^{51}$V NMR spectra of (ImH)[L$^1$OV-($\mu$-O)-VOL$^2$] (**2**) in $CD_3CN$/toluene (1:2 v/v) solution at variable temperatures.

**$^{51}$V NMR Spectroscopy.** To understand more about the solution structures of $\mu$-oxo divanadium(IV,V) complexes, $^{51}$V NMR spectra of the compounds **1**−**3** have been measured in $CD_3CN$/toluene (1:2 v/v) solution over a range of temperatures (298−220 K). Almost identical features are obtained in all cases and typical spectra for **2** are shown in Figure 7. At room temperature, two signals are obtained, both in the diamagnetic chemical shift region (Figure 7a). One of these is sharp (peak I), appearing at −356 ppm while the other at −460 ppm (peak II) has a broad feature with a peak area ratio (peak I: peak II) of ca. 4.1. This again is in accord with the two different structural forms of compound **2** in solution at room temperature as shown by eq 3. The one with a bent V−O−V bridge has a less shielded vanadium(V) center that probably appears as a sharp peak (peak I), while the other form with a linear V−O−V bridge produces a more shielded vanadium(V) center with a broad NMR signature (peak II) at a higher field due to greater delocalization of the odd electron. As the temperature is lowered to 240 K, line broadening occurs for both peaks (Figure 7b) possibly due to slowing of the electronic relaxation rate. The peak area ratio (peak I:peak II) decreases to ca. 3.0 at this temperature, indicating a shift of the equilibrium (eq 3) to the right-hand side due to pronounced solvation effects. At still lower temperatures due to the decrease of the intramolecular thermal electron-transfer rate the odd electron gets virtually trapped at one vanadium center. The spectrum recorded at ca. 220 K (Figure 7c) shows a single peak in the downfield region (−360 ppm) with a broad feature, indicating that at this

---

(27) Gagné, R. R.; Koval, C. A.; Smith, T. J.; Cimolino, M. C. *J. Am. Chem. Soc.* **1979**, *101*, 4571.

(28) Dupeyre, R. M.; Lemaire, H.; Rassat, A. *J. Am. Chem. Soc.* **1965**, *87*, 3771.

(29) Slichter, C. P. *Phys. Rev.* **1955**, *99*, 478.

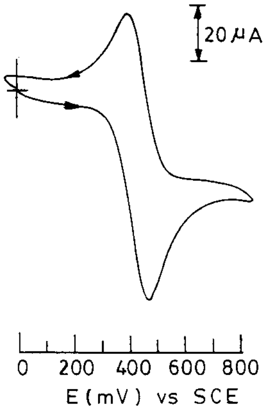

**Figure 8.** Cyclic voltammogram of (ImH)[L$^1$OV-($\mu$-O)-VOL$^1$] (**3**) in CH$_3$CN (0.1 M TEAP) at a platinum-disk electrode; scan rate 50 mV s$^{-1}$ and potentials recorded vs SCE.

temperature the electronic structures of the two species differ very little due to localization of the unpaired electron.

**UV−Vis Spectra and Electrochemistry.** The electronic spectra of **2** and **3** have similar features, each displaying a number of bands in CH$_3$CN solution as summarized in the Experimental Section. The spectrum of **2** shows a new band of moderate intensity $\epsilon = 1600$ M$^{-1}$ cm$^{-1}$ (1480 M$^{-1}$ cm$^{-1}$ for **3**) in the near-IR region at 965 nm (970 nm for **3**) not found in the precursor complexes[13] which can be assigned to an intervalence transfer (IT) transition between the participating vanadium centers. In scrupulously dried solvents, intensity of this IT band remains practically unchanged for at least over a couple of hours. Results clearly rule out any possibility of these mixed-oxidation compounds being dissociate into mononuclear vanadium(IV) and -(V) counterparts under moisture free condition.[7] In the visible region, the spectrum also contains a broad shoulder centered at 750 nm (740 nm for **3**) composed of more than one band due to ligand-field transitions. The intensity of this d−d transition(s), $\epsilon = 950$ M$^{-1}$ cm$^{-1}$ (900 M$^{-1}$ cm$^{-1}$ for **3**), is considerably higher than observed for the mononuclear vanadium(IV) precursors[13] due to intensity borrowing from the adjoining IT band. The remaining strong band at 396 nm, $\epsilon =$ 15 500 M$^{-1}$ cm$^{-1}$ (389 nm, 14 300 M$^{-1}$ cm$^{-1}$ for **3**) arises from the PhO$^-$ → V(d$\pi$) LMCT transition, as previously observed for the mononuclear vanadium(IV) counterparts.[13] All remaining bands appearing in the UV region are due to ligand internal transitions.

The redox properties of the mixed-valence complexes (**2** and **3**) have been examined by cyclic voltammetry using a platinum working and SCE reference electrodes. Figure 8 depicts a representative voltammogram (**3**) in acetonitrile solution (0.1 M TEAP) which reveals a one-electron oxidation (V$^{IV}$V$^V$/V$^V$V$^V$) with $E_{1/2} = 0.42$ V and conforms to the criteria for Nernstian-reversibility ($\Delta E_p$ remains practically constant within an accuracy of ±1.0% regardless of the scan rate in the range 50−500 mV s$^{-1}$; the current function, $i_p/v^{1/2}$, is independent of scan rate and $i_{pa}/i_{pc} \cong 1$).[30] Identical features are obtained for **2** ($E_{1/2}$ $= 0.44$ V and $\Delta E_p = 75$ mV). Comparison with the ferrocene/ferrocenium couple as an internal standard ($\Delta E_p = 85$ mV) suggests this process to be monoelectronic (eq 4).

$$[\mathrm{LOV^{IV}\text{-}(\mu\text{-}O)\text{-}V^{V}OL}]^- \underset{E_{1/2} = 0.42\ \mathrm{V}}{\overset{-e^-}{\rightleftharpoons}} [\mathrm{LOV^{V}\text{-}(\mu\text{-}O)\text{-}V^{V}OL}]^0 \qquad (4)$$

The electron stoichiometry for this process was further examined by oxidative controlled-potential electrolysis with a platinum-gauze working electrode ($E_w = 0.6$ V). The results show the consumption of 1.0 ± 0.1 F of charge per mole of complexes.

## Concluding Remarks

The mixed-oxidation divanadium(IV,V) complex (ImH)[L$^1$-OV-($\mu$-O)-VOL$^2$] (**2**) containing two dissimilar ligands (L$^1$ and L$^2$) attached to the vanadium centers has been reported. In the solid state, compound **2** possesses crystallographically imposed mirror symmetry which is quite unusual considering the syn angular structure of its [V$_2$O$_3$]$^{3+}$ core.[11,13] This is due to the presence of a dimeric structure with bromine atom disordered over the two ligand sites (one-half occupancy). In CH$_3$CN/toluene (1:2 v/v) solution, EPR spectra of **2** and **3** at room temperature have 15-line features with asymmetric distortions. Similar asymmetry is not observed in the EPR spectra of divanadium(IV,V) compounds with octahedral vanadium sites.[4,6b] For divanadium(IV,V) compounds with square-pyramidal vanadium centers such as in **1**−**3**, asymmetric EPR features in acetonitrile solution probably arise from a temperature dependent solvation process involving an equilibrium between the two structural forms containing magnetically inequivalent syn angular and anti linear [V$_2$O$_3$]$^{3+}$ cores. EPR spectra in noncoordinating solvents and $^{51}$V NMR study at variable temperatures also support this structural equilibrium in solution.

**Acknowledgment.** Financial support received from the Council of Scientific and Industrial Research, New Delhi and the Ministry of Science and Technology, Korea are gratefully acknowledged. Part of this work has been carried out partially for the KOYOU projects at the KBSE from 1996 to 1998. We thank Professor K. Nag at IACS for many helpful discussions and Ms. Seen Ae Chae at the KBSE for technical support on NMR experiments.

**Supporting Information Available:** A unit cell packing diagram of (ImH)[L$^1$OV-($\mu$-O)-VOL$^2$] (**2**) and an X-ray crystallographic file, in CIF format, for **2** are available free of charge via the Internet at http://pubs.acs.org.

IC980743+

---

(30) Brown, E. R.; Large, R. F. Electrochemical Methods. In *Physical Methods in Chemistry*; Weissberger, A., Rossiter, B., Eds.; Wiley-Interscience: New York, 1971; Part IIA, Chapter VI.